Class. Quantum Grav. **19** (2002) 1925–1933 PII: S0264-9381(02)30095-9

Status report and near future prospects for the gravitational wave detector AURIGA

J-P Zendri[1], L Baggio[2], M Bignotto[3], M Bonaldi[4], M Cerdonio[3], L Conti[3], M De Rosa[7], P Falferi[4], P L Fortini[6], M Inguscio[7], A Marin[3], F Marin[7], R Mezzena[2], A Ortolan[5], G A Prodi[2], E Rocco[2], F Salemi[6], G Soranzo[1], L Taffarello[1], G Vedovato[5], A Vinante[2] and S Vitale[2]

[1] Istituto Nazionale di Fisica Nucleare INFN, Sezione di Padova, Via Marzolo 8, I-35131, Padova, Italy
[2] Department of Physics, University of Trento and INFN, Gruppo Coll. di Trento Sezione di Padova, I-38050 Povo, Trento, Italy
[3] Department of Physics, University of Padova and INFN, Sezione di Padova, Via Marzolo 8, I-35131, Padova, Italy
[4] Centro CeFSA, ITC-CNR, Trento and INFN, Gruppo Coll. di Trento Sezione di Padova, I-38050 Povo, Trento, Italy
[5] INFN National Labs of Legnaro, Via Romea 4, I-35020 Legnaro, Padova, Italy
[6] Department of Physics, University of Ferrara and INFN, Sezione di Ferrara, I-44100 Ferrara, Italy
[7] Department of Physics, University of Firenze and INFN, Sezione di Firenze, I-50125 Arcetri, Firenze, Italy

E-mail: zendri@lnl.infn.it

Received 26 October 2001, in final form 28 November 2001
Published 18 March 2002
Online at stacks.iop.org/CQG/19/1925

Abstract
We describe the experimental efforts to set up the second AURIGA run. Thanks to the upgraded capacitive readout, fully characterized and optimized in a dedicated facility, we predict an improvement in the detector sensitivity and bandwidth by at least one order of magnitude. In the second run, AURIGA will also benefit from newly designed cryogenic mechanical suspensions and the upgraded data acquisition and data analysis.

PACS number: 0480N

(Some figures in this article are in colour only in the electronic version)

1. Introduction

The first AURIGA run ended in November 1999 because of a cryogenic failure. This forced us to warm up the detector to room temperature. During the two years of data acquisition the detector reached the best strain sensitivity of $S_{hh}^{1/2} \approx 4 \times 10^{-22}\ \mathrm{Hz}^{-1/2}$ within a bandwidth of $\sim$2 Hz around the two resonant frequencies (911 and 929 Hz) [1] and duty cycle of $\sim 1/3$ of

0264-9381/02/071925+09$30.00

the total acquisition time. For an impulsive signal the AURIGA noise level corresponds to a minimal detectable Fourier transform amplitude of $H_0 \approx 2.5 \times 10^{-22}$ Hz^{-1}. Although the above sensitivity is among the best ever achieved, for the second AURIGA run we plan to use an upgraded readout optimized to widen the bandwidth to several tens of Hz. Thus we expect to increase the amplitude sensitivity by at least a factor of 10.

To understand the pursued strategy let us model the resonant bar first longitudinal mode as a harmonic oscillator of equivalent mass M_{eff} and resonant frequency ω_b. An incoming gravitational wave of amplitude $h(t)$ drives the resonator with a force $F_{grav} \propto \ddot{h}(t)$ [2] and the induced oscillator displacement, which is the physical observable, contains all the information about the wave amplitude. The detector sensitivity is affected by at least two unavoidable displacement noise sources. The first comes from the amplifier stage and is described by two partially correlated noise generators; (i) the equivalent displacement noise generator x_n and (ii) the back-action noise force generator F_{ba} which randomly drives the oscillator motion. The power spectra of the back-action noise $S_{F_{ba}F_{ba}}$ and the displacement noise $S_{x_n x_n}$ scale as α^2 and α^{-2}, respectively [3], where α is the transduction efficiency, defined as the ratio between the displacement-induced electrical signal measured at the amplifier input and the mechanical oscillator motion amplitude. According to quantum mechanics predictions neither of these two noise power spectra can vanish as they must satisfy the inequality $S^{1/2}_{F_{ba}F_{ba}} \times S^{1/2}_{x_n x_n} \geqslant \hbar/2$ [4]. In practice real amplifiers operate $N_\hbar \sim 10^2$–10^4 times above this level. Thus in order to improve the sensitivity the first requirement for a readout is to employ amplifiers which operate as close as possible to the quantum limiting value $N_\hbar = 1$. The best value achieved for the first AURIGA run using a commercial dc-SQUID as the first amplification stage was $N_\hbar \approx 4000$, while as discussed below, for the second run we will employ a two-stage SQUID amplifier which approaches $N_\hbar \approx 100$.

The second unavoidable noise source affecting the detector sensitivity is the thermal noise which is described by the Langevin force F_{Th} with power spectrum $S_{F_{Th}F_{Th}} = 2k_B T M_{eff}\omega_b/Q_b$, where k_B is the Boltzmann constant, Q_b is the harmonic oscillator quality factor and T its temperature. Both back-action and Langevin noise sources act on the mechanical resonator as disturbance forces that limit the sensitivity to the gravitational force F_{grav}. To include all the noise sources in the sensitivity analysis we define the equivalent displacement noise force generator $F_{n\text{-}eq}$ as the noise force generator which produces at the output port the measured displacement noise x_n. Thus the force generator noise power spectrum is defined as $S_{F_{n\text{-}eq}F_{n\text{-}eq}} = S_{x_n x_x}/|G(\omega)|^2$, where $G(\omega) = M_{eq}^{-1}\left(\omega_b^2 - \omega^2 + \mathrm{i}\,\omega_b\omega/Q_b\right)^{-1}$ is the transfer function of the oscillator force. In figure 1 the power spectrum of the noise forces is plotted; the total noise curve which is the sum of all components is also shown. Figure 1 shows that, in general, any increase of the transduction efficiency α is accompanied by an increase in both the bandwidth and the sensitivity; the lower level of the total noise curve is dominated by the α-independent thermal noise contribution while $S_{F_{n\text{-}eq}F_{n\text{-}eq}}$ decreases as α^{-2}. When the transduction efficiency becomes very high the minimum of the total noise curve is dominated by the back-action contribution and therefore it scales as α^2. At this point, any further increase in α corresponds to widening the detector bandwidth without improving its sensitivity. However, as this limit condition is far from being achieved [3], we have to maximize the transduction efficiency in order to optimize the readout.

In section 2.1, we describe our efforts to meet the above requirements (minimization of $N_\hbar$ and maximization of α) and the state of the art. Section 2.2 is devoted to the description of the new cryogenic suspension developed to fully exploit the bandwidth increase and section 2.3 to the upgrades of the detector cryogenics. In section 2.4, we report the expected sensitivity for the second run. Finally, in section 2.5, we outline the new features of the data acquisition and analysis.

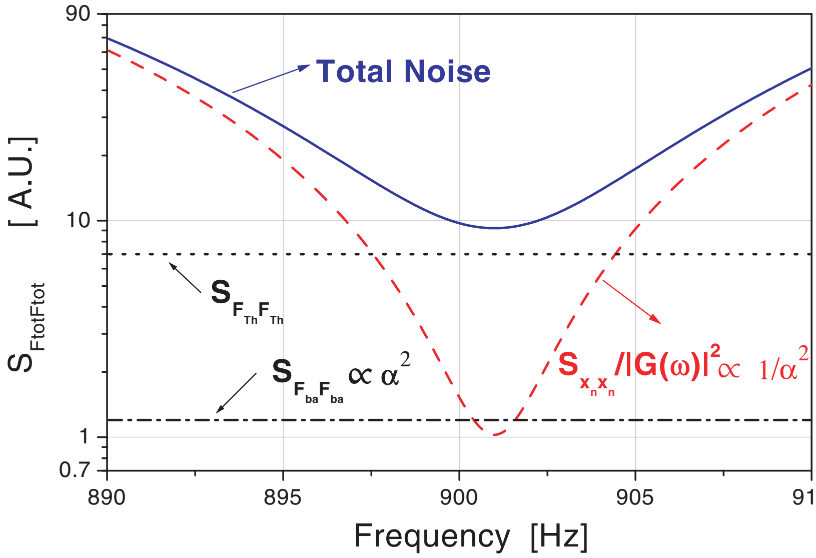

Figure 1. Power spectrum of the noise forces acting on the single-mode resonant detector. The dashed line, which scales as α^{-2}, is the contribution coming from the amplifier broadband displacement noise, the dotted line the thermal noise contribution and the dot-dashed line the back-action contribution, which scales as α^2. The overall noise curve (filled line), which is the sum of all the above components, is also plotted.

2. The second AURIGA run

2.1. Transduction and amplification

In the second run, the AURIGA detector will be equipped with a resonant capacitive transducer read by a two-stage SQUID amplifier. To maximize the signal transfer from the transducer output to the SQUID input coil, a high turn ratio superconducting transformer is inserted between them. The transducer capacitance C and the transformer primary coil form an electrical resonator with resonant frequency $\omega_{el} = (L_{eff}C)^{-1/2}$, where $L_{eff} = L\big(1 - k^2 L_s/(L_s + L_{in})\big), k^2 = M^2/(LL_s)$, is the transformer geometrical coupling, M the transformer mutual inductance, L_{in} the SQUID input coil self-inductance, L and L_s, respectively, the primary and the secondary coil inductances of the transformer. For this experimental set-up and assuming that the electrical resonant frequency is far from the mechanical resonant frequencies ω_{mec} the frequency-dependent transducer efficiency α_{Cap} becomes approximately

$$\alpha_{Cap} = \frac{M E_0 \omega}{L_{eff}(L_s + L_{in})} \frac{1}{\omega_{el}^2 - \omega^2 + \mathrm{i}\omega_{el}\omega/Q_{el}} \quad \left[\frac{A}{m}\right] \tag{1}$$

where E_0 is the transducer electric bias field and Q_{el} the electric resonator quality factor.

When $\omega_{el} \gg \omega_{mec}$, as in the first AURIGA run, the above formula, for the optimal condition $L_{in} \approx L_s$, takes the simple form $\alpha_{Cap} = E_0\omega k C^{1/2}\big/\big(2\omega_{el}^2\sqrt{L_{in}}\big)$, which states that, given any electrical resonance ω_{el}, the way to maximize the transduction efficiency is to maximize the transducer bias field and capacitance and the transformer geometrical coupling k. An improvement of at least one order of magnitude in both the first two parameters is the main goal of the present research and development programme on the capacitive transducer. However, as this programme is still in progress, the second AURIGA run will

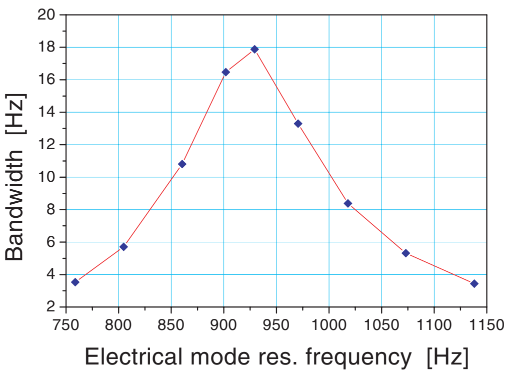

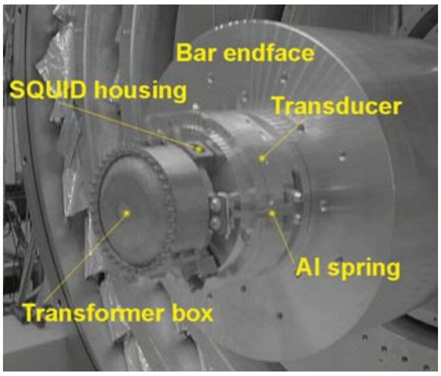

Figure 2. Left: the overall detector bandwidth calculated for different electrical resonance frequencies. The mechanical resonance is at 920 Hz while the amplifier used is a single dc-SQUID. Right: picture of the new transduction line connected to the bar endface. It is possible to see the capacitive transducer which through an aluminium spring is mechanically connected to the superconducting box (a deposition of Sn–Pd over a copper core) which contains both the superconducting matching transformer and the two SQUIDs.

employ an alternative method to maximize α. Indeed, as suggested by equation (1), by equating the electrical mode resonant frequency to the mechanical one a huge increase of the transduction efficiency is expected around the frequencies where the gravitational wave-induced displacement is largest. The soundness of this procedure becomes evident in figure 2 where the calculated detector bandwidth is plotted for different values of ω_{el} and reaches its maximum value when the mechanical and the electrical modes are tuned. The drawback of this procedure is that it requires a very high electrical quality factor $\left(Q_{el} \approx 10^6\right)$ to preserve high sensitivity and strong rejection of electromagnetic interferences. To meet both these conditions the superconducting transformer is assembled with intrinsically low-loss dielectric materials and housed in a superconducting box designed by finite element methods (FEM) to avoid spurious mechanical resonances in the frequency range of interest.

Even with the predicted improvement of the transduction efficiency the transducer for the next AURIGA run will still be resonant with the bar oscillator. However, as a consequence of the increment of α, less mechanical amplification is required and thus the transducer resonant plate can be made heavier with a consequent bandwidth improvement. Indeed, the optimal transducer mass is now [5] about 4 kg, 10 times bigger than the one used in the previous run. The new transducer was designed using FEM to avoid spurious resonances and to keep the internal-stress gradient as low as possible (in order to reduce thermoelastic losses). Basically it has the usual mushroom geometry [6] with the central part of the membrane thinned to match the requirement of high mass and resonant frequency tuned to that of the bar (≈900 Hz).

The second requirement for an optimal transduction chain is to incorporate an amplifier stage operating near the quantum limited energy sensitivity ($N_\hbar = 1$). In principle, in our frequency range a SQUID amplifier can approach this limit. However, the noise level of the single SQUID amplifier is strongly affected by the room temperature electronics which adds a temperature-independent noise contribution. In order to overcome this problem we developed a two-stage SQUID in which the sensor SQUID voltage output is amplified by a second low-noise SQUID. This two-stage SQUID was demonstrated to work in the temperature range between 4.2 K and 50 mK with a broadband noise power spectrum which scales linearly with the thermodynamic temperature, as expected for intrinsic noise-limited SQUID, down to 300 mK [7]. When coupled to a high quality factor electrical resonator the measured energy sensitivity of the device at 4.2 K was about $N_\hbar = 420$, linearly decreasing with temperature to $N_\hbar = 200$ at 1.5 K [8]. The energy sensitivity at lower temperature has still to be investigated. As the two-stage SQUID is based on a commercial device with the input coil strongly coupled to the SQUID loop, it is particularly suitable for the integration in a high sensitive transducer chain and thus will be employed in the second AURIGA run.

The massive transducer, coupled to the high-Q transformer and read by the two-stage SQUID amplifier, was tested in the transducer test facility within the temperature range 1.6–4.2 K. The detailed results of these measurements are described elsewhere [9]. Let us just note here that the tested transduction chain, assembled as it will operate in the AURIGA detector, operated with an amplifier energy resolution ($N_\hbar = 350$ at 1.6 K) not too far from the SQUID noise level measured in bench tests. The measured electrical quality factor, $Q_{el} = 10^6$, the absence of any measurable electromagnetic interference contribution and the obtained high geometrical coupling $k = 0.86$ meet the requirements. Finally, differently from the previous run, the superconducting transformer and the SQUID housing box are placed close to the transducer (see figure 2) with the aim of reducing microphonicity noise. Thanks to the softness of the connection, given by Al springs, this operation does not affect the transducer mechanical quality factor, which at cryogenic temperature turns out to be $Q_t = 1.4 \times 10^6$.

2.2. Suspensions

To exploit the predicted sensitivity and bandwidth improvement, in the second run AURIGA will be equipped with a new cryogenic suspension, optimized for broadband operation. The main mechanical filter is a cascade of six ‘spring-mass’ elements forming together a column of 25 cm diameter and 80 cm length (total mass 130 kg). Each spring element, which at 1 kHz should provide an attenuation of −40 dB, is designed to operate with a static internal stress less than 25% of the yield stress of the material (the high strength aluminium alloy ‘alumold 1-500’). Basically it is composed of three ‘C’ shaped elements machined in a single piece in a ‘trefoil’ configuration, which provides a good attenuation in all six degrees of freedom. The brass masses of the single suspension element are bolted to the spring monolithic piece. According to the FEM prediction, the vertical resonant frequency should be 95 Hz while no other internal resonances should appear in the frequency window 200–1800 Hz. The assembling of the new suspensions and their connections to the old AURIGA cryostat are described in figure 3.

Another interesting feature of the new suspension system is the bar hanging method. Instead of the old belly cable around the bar middle section, the bar will hang from its centre of mass by a tubular cable. The tubular geometry has been chosen in order to maintain the longitudinal mechanical attenuation while avoiding the presence of the violin modes in the frequency range of interest. The expected advantages of this procedure are an improvement of attenuation and the bar quality factor as a consequence of the lower coupling between the bar longitudinal mode and the suspension motion [10].

The simulation by finite elements modelling software predicts an overall attenuation of 300 dB at 1 kHz without any expected internal resonance in the frequency window between 700 and 1200 Hz. At the moment of writing almost all the new suspension parts have been delivered and tests are being performed.

2.3. Cryogenics

As expected, the ultracryogenic detectors achieved a better sensitivity level with respect to warmer resonant detectors. However, this advantage was achieved at the cost of a decreased

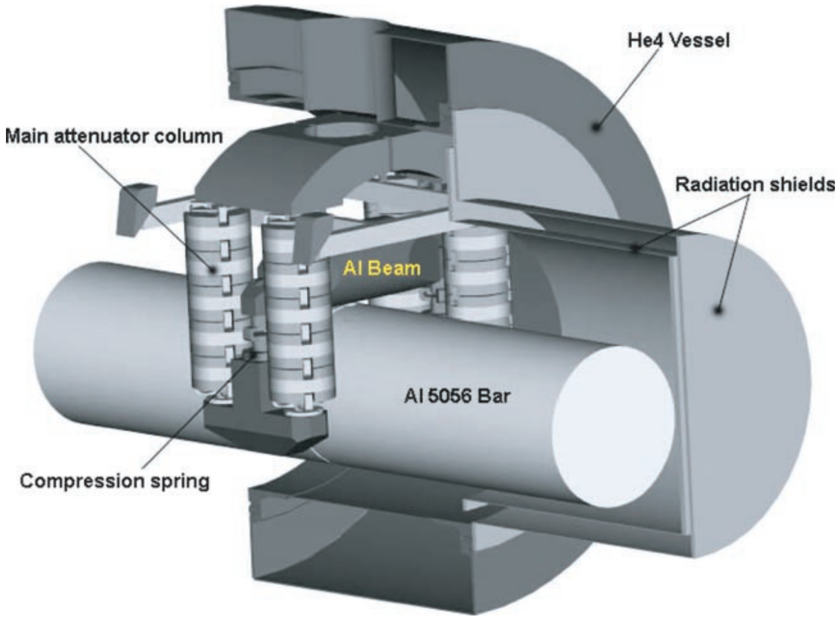

Figure 3. Cross section of the new AURIGA cryogenic suspensions. The 4 K vessel of the cryostat supports a stainless steel frame, from which the whole suspension system is hung. The four main suspension columns are fixed to a big 300 kg 'D-shaped' aluminium mass, supported by four titanium springs. The aim of these four springs is to uncouple the steel frame from the columns. Each pair of columns supports an inverted 'T' aluminium mass on the top of which is fixed a compression spring with an upper conical join which is used to lean an aluminium beam. The bar hangs at its centre of mass with a tubular cable which is attached with a 'bayonet' mount to the aluminium beam. The insertion point into the antenna has been designed with a conical joint surface at an angle of 45°. The contact area of the two surfaces guarantees a good thermal link for the antenna.

duty cycle [11]. This is due to poor reliability of the ^{3}He–^{4}He dilution refrigerator. In addition, the refrigerator 1 K-pot has been demonstrated to be a source of mechanical disturbance, blinding the detector during the daily refill. Given this we have decided to split the second AURIGA run into two phases. During the first one the dilution refrigerator will be substituted by a ^{4}He pumped dewar with a capability of about 150 liters. This operation is expected to achieve a stable cryogenic point at 1.5 K. In the second phase, a modified dilution refrigerator will be added to reach the lowest temperatures. In particular, a new 1 K-pot is being designed using FEM analysis to avoid any internal resonance in the kHz frequency region. Furthermore, the new 1 K-pot will incorporate the recently developed recipes to avoid its vibrational noise[8].

2.4. Expected sensitivity

In table 1 we report the main dynamic parameters used for the calculation of the sensitivity for the second AURIGA run. The transducer and the electronic readout parameters as well as the values of the two SQUID noise power spectra are those actually measured in the transducer test facility. The bar parameters are the same as those obtained in the previous run except for

[8] A Raccanelli, Max Plank Institute für Radioastronomie, Bonn (D), private communication.

Table 1. Table of the relevant parameters used for the calculation of the sensitivity curve of figure 4. The parameters come from the measurements in the transducer test facility or the previous AURIGA run.

Parameter	Symbol	Value
Bar mass	m_b	2230 kg
Bar length	L_b	2.93 m
Bar resonant frequency	$\nu_b = \omega_b/2\pi$	902 Hz
Bar quality factor	Q_b	8×10^6
Transducer mass	m_t	4.0 kg
Transducer resonant frequency	$\nu_t = \omega_t/2\pi$	909 Hz
Transducer quality factor	Q_t	1.5×10^6
Transducer bias field	E_0	10^7 V m^{-1}
Primary coil inductance	L	6.5 H
Secondary coil inductance	L_s	3.2 μH
Transformer mutual inductance	M	3.8 mH
SQUID input coil	L_{in}	1.8 μH
SQUID mutual inductance	M_{sq}	10 nH
Electrical quality factor	Q_{el}	10^6

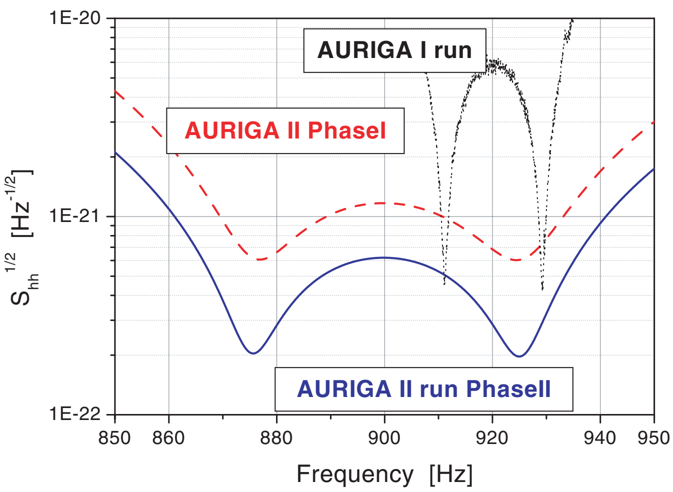

Figure 4. The predicted sensitivity curve for the second AURIGA run. The dashed line corresponds to the first phase with the detector operating at 1.5 K and the filled line with the detector operating at 0.1 K. For comparison the sensitivity obtained for the first AURIGA run is also reported (dotted line).

the bar resonant frequency, which is lowered by the presence of a more massive transducer basement[9].

The sensitivity curves expected for the two phases of the second run are plotted in figure 4; for comparison the sensitivity measured in the previous AURIGA run is also plotted. They can be used to calculate the pulse Fourier amplitude H_{min} at $S/N = 1$. For the first phase we get $H_{min} = 6 \times 10^{-23}$ Hz^{-1}, which corresponds to a bar absorbed energy E_{min} five times higher

[9] We calculate the expected resonant frequency according to the empiric formula [12], which states that any mass connected to the bar endface reduces the resonant frequency of about 0.3 Hz kg^{-1}. However, the real value will soon be estimated measuring, at room temperature, the frequencies of the transducer–bar two-mode system.

than the minimum achievable [13] using an $N_\hbar = 350$ SQUID amplifier (as our two-stage SQUID at 1.5 K). This result suggests that although we have optimized the transduction chain the thermal noise is still very important.

For phase II, the predicted (but not optimized) minimal detectable amplitude of $H_{min} = 2.5 \times 10^{-23}$ Hz^{-1} corresponds to an energy resolution of about 250 $\hbar\omega_b$, more than twice the minimum achievable. However, unlike the phase I curve, which was predicted using already measured parameters, the phase II curve is drawn using a SQUID back-action power spectrum value which is the extrapolation to 0.1 K of that measured in the temperature range 1.5–4.2 K. The measurements of the SQUID noise properties at ultracryogenic temperature will be performed in the near future.

Finally, a sensitivity improvement should be obtained reducing the thermal noise level, for instance increasing the bar quality factor, or reducing its effect through the increase of the transduction efficiency. Both these advantages should already be obtained during phase I of the run, thanks to the new design of the mechanical suspensions and to the incremented transducer bias field.

2.5. Data acquisition and data analysis

The data acquisition and data analysis systems have been fully redesigned and upgraded to satisfy the new requirements of the second AURIGA run (wider bandwidth and higher sensitivity) and to allow the operation of AURIGA in an intercontinental network of bar and interferometric gw detectors [14]. To meet these requirements, we have adopted the FRAME format (developed by VIRGO/LIGO) for the Input/Output and for future data exchange. The PC Linux, the open source tools and libraries and the C++ programming language have been the natural choice for the development platform. We have developed two libraries: (i) the process control library (PCL) aimed at managing communications and controls of the user processes and (ii) the AURIGA algorithm library (AAL) which gathers the specific algorithms of the AURIGA analysis (adaptive filters, template matching, trigger extraction). The AAL library also addresses the problems of unbiased estimation of signal parameters and the set-up of the data quality and data validation procedures. We are also developing an interactive tool of data analysis based on CINT/ROOT for data monitoring and diagnostic purposes.

3. Conclusions

In the next few months the AURIGA detector will start its second acquisition run. Thanks to the upgraded transduction chain, already tested on the test facility, an improvement of about a factor of 10 in amplitude sensitivity is expected. In terms of energy resolution this corresponds to only a few hundred times the fundamental standard quantum limit. An attempt to increase the duty cycle and to understand the origin of the non-stationary noise will be made by splitting the second run into two different phases. During the first phase the detector will operate at 1.5 K, which should favour a stable and quiet cryogenic condition. In the second phase, the detector will operate at ultracryogenic temperature using an upgraded dilution refrigerator optimized for long-term and quiet operation. Finally, an improvement in both sensitivity and duty cycle is expected from the use of the new suspensions optimized for broadband operation. The upgraded AURIGA detector with the new data analysis will also be ready to join the interferometric network of gravitational wave detectors.

References

[1] Zendri J P *et al* 2000 *Gravitational Waves, Proc. 3rd E Amaldi Conf. (CalTech, CA, 1999)* ed S Meshkov (New York: AIP) p 421

[2] See for instance Misner C W, Thorne K S and Wheeler J A 1973 *Gravitation* (New York: Freeman)

[3] Zendri J P *et al* 2002 *Recent Developments in General Relativity, Proc. 14th Congress on General Relativity (Genova, Italy, Sept. 2000)* (Berlin: Springer) pp 285–99 at press

[4] Caves C M 1982 *Phys. Rev.* D **26** 1817

[5] Crivelli Visconti V 1999 *PhD Thesis* University of Padova webpage http://www.auriga.lnl.infn.it

[6] Rapagnani P 1982 *Nuovo Cimento* C **5** 385

[7] Mezzena R *et al* 2001 *Rev. Sci. Instrum.* **72** 3694

[8] Vinante A *et al* 2002 *Proc. of the 4th Edoardo Amaldi Conf. on Gravitational Waves (Perth, Western Australia, 8–13 July 2001) Class. Quantum Grav.* **19** 1979

[9] Marin A *et al* 2002 *Proc. of the 4th Edoardo Amaldi Conf. on Gravitational Waves (Perth, Western Australia, 8–13 July 2001) Class. Quantum Grav.* **19** 1991

[10] Coccia E 1984 *Rev. Sci. Instrum.* **55** 1980

[11] Astone P *et al* 2002 *Proc. of the 4th Edoardo Amaldi Conf. on Gravitational Waves (Perth, Western Australia, 8–13 July 2001) Class. Quantum Grav.* **19** 1367

[12] Paoli S 1993 *Graduate Thesis* University of Padova

[13] Price J C 1987 *Phys. Rev.* D **36** 3555

[14] Ortolan A *et al* 2002 *Proc. of the 4th Edoardo Amaldi Conf. on Gravitational Waves (Perth, Western Australia, 8–13 July 2001) Class. Quantum Grav.* **19** 1457